

This is an Open Access document downloaded from ORCA, Cardiff University's institutional repository: <https://orca.cardiff.ac.uk/id/eprint/173057/>

This is the author's version of a work that was submitted to / accepted for publication.

Citation for final published version:

Ji, Haoran, Zheng, Yuxin, Yu, Hao, Zhao, Jinli, Song, Guanyu, Wu, Jianzhong and Li, Peng 2024. Asymmetric bargaining-based SOP planning considering peer-to-peer electricity trading. *IEEE Transactions on Smart Grid* 10.1109/tsg.2024.3471611

Publishers page: <https://doi.org/10.1109/tsg.2024.3471611>

Please note:

Changes made as a result of publishing processes such as copy-editing, formatting and page numbers may not be reflected in this version. For the definitive version of this publication, please refer to the published source. You are advised to consult the publisher's version if you wish to cite this paper.

This version is being made available in accordance with publisher policies. See <http://orca.cf.ac.uk/policies.html> for usage policies. Copyright and moral rights for publications made available in ORCA are retained by the copyright holders.



# Asymmetric Bargaining-Based SOP Planning Considering Peer-to-Peer Electricity Trading

Haoran Ji, *Senior Member*, IEEE, Yuxin Zheng, Hao Yu, *Senior Member*, IEEE, Jinli Zhao, *Member*, IEEE, Guanyu Song, *Senior Member*, IEEE, Jianzhong Wu, *Fellow*, IEEE, and Peng Li, *Senior Member*, IEEE

**Abstract**—The flexible power distribution devices, represented by soft open points (SOPs), can facilitate power exchange among regional distribution networks. However, given the substantial investment in SOPs, there exists an urgent need for their reasonable configuration and fair allocation among multi-stakeholders. Promisingly, the peer-to-peer (P2P) electricity trading based on SOPs can not only effectively reduce operational cost, but also impart revenue-generating abilities to SOP investment. Aiming at the optimal SOP configuration under multi-stakeholder investment, this paper proposes an asymmetric bargaining-based planning method for SOPs considering P2P trading. First, a planning-operation two-layer coupling framework of SOPs is established under multi-stakeholder games. In the planning layer, analyzing the game behaviors among multiple distribution companies (DISCOs), an asymmetric bargaining-based planning model is formulated to obtain the configuration and investment schemes of SOPs. In the operational layer, the P2P trading and the profitability of multiple DISCOs are driven by price incentives. Then, a two-layer coupling model is built and efficiently solved using the generalized Benders decomposition algorithm. Finally, the effectiveness of the proposed method is validated on a practical distribution network. The proposed method incentivizes investment in SOPs by balancing the interests of multiple DISCOs, while efficiently improving the operational performance of distribution networks.

**Index Terms**—Distribution networks (DNs), soft open points (SOPs), asymmetric bargaining-based planning, peer-to-peer (P2P) electricity trading

## NOMENCLATURE

### Sets

$\Omega_k^N, \Omega_k^{\text{Line}}$	Set of all nodes/lines at area $k$
$\Omega^R$	Set of all areas
$\Omega^{\text{SOP}}$	Set of all SOPs to be planned
$\Omega_k^{\text{SOP}}, \Omega_k^{\text{SOP,Line}}$	Set of SOPs/tie-lines planned at area $k$
$\Omega_m^{\text{AC}}$	Set of converters planned for $m$ -th SOP

### Indexes

$i, j$	Indexes of nodes
$ij$	Index of lines
$t$	Index of time periods
$k$	Index of areas

This work was supported by the National Natural Science Foundation of China (U22B20114, 52277117). (*Corresponding author: Hao Yu*)

H. Ji, Y. Zheng, H. Yu, J. Zhao, G. Song and P. Li are with the Key Laboratory of Smart Grid of Ministry of Education, Tianjin University, Tianjin 300072, China (email: jihaoran@tju.edu.cn; yxzheng@tju.edu.cn; tjyuh@tju.edu.cn; jlzhao@tju.edu.cn; gysong@tju.edu.cn; lip@tju.edu.cn).

J. Wu is with the Institute of Energy, School of Engineering, Cardiff University, Cardiff CF24 3AA, U.K. (email: wuj5@cardiff.ac.uk).

$\omega$	Index of scenarios
$m$	Index of SOPs
$n$	Index of constraints
<b>Variables</b>	
$C_m^{\text{SOP}}, C_m^{\text{SOP,O}}$	Annual investment/maintenance cost of $m$ -th SOP
$R_k^P$	Annual cooperative surplus shared for DISCO $k$
$C_k^I, C_k^{\text{Line}}$	Annual SOP/tie-line investment cost of DISCO $k$
$C_k^O, C_k^S$	Annual maintenance/land expropriation cost of DISCO $k$
$C_k^G, C_k^{\text{P2P}}$	Annual trading cost with upper grid/P2P paid by DISCO $k$
$C_k^U$	Annual voltage deviation cost of DISCO $k$
$\pi_{\omega,k,t}^P, \pi_{\omega,k,t}^Q$	P2P trading price of active/reactive power at area $k$ in period $t$ during scenario $\omega$
$P_{\omega,i,t}^{\text{SOP}}, Q_{\omega,i,t}^{\text{SOP}}$	Active/reactive power injected by SOP at node $i$ in period $t$ during scenario $\omega$
$P_{\omega,m,k,t}^{\text{SOP}}, Q_{\omega,m,k,t}^{\text{SOP}}$	Active/reactive power injected by $m$ -th SOP at area $k$ in period $t$ during scenario $\omega$
$P_{\omega,k,t}^{\text{B,g}}, P_{\omega,k,t}^{\text{S,g}}$	Active power purchased/sold with upper grid of area $k$ in period $t$ during scenario $\omega$
$V_{\omega,i,t}^{\text{dev}}$	Indicator of voltage deviation at node $i$ in period $t$ during scenario $\omega$
$P_{\omega,i,t}^{\text{LD}}, Q_{\omega,i,t}^{\text{LD}}$	Active/reactive power consumption at node $i$ in period $t$ during scenario $\omega$
$\varpi_{\omega,k,t}$	Power supply to demand ratio of area $k$ in period $t$ during scenario $\omega$
$\mu_{m,k}$	Investment ratio for $m$ -th SOP of DISCO $k$
$p_\omega$	Probability of scenario $\omega$
$P_{\omega,ij,t}, Q_{\omega,ij,t}$	Active/reactive power flow of line $ij$ in period $t$ during scenario $\omega$
$S_{m,i}^{\text{SOP}}$	Capacity of $m$ -th SOP connected to node $i$
$E_k^B, E_k^S$	Total active power purchased/sold by DISCO $k$ in P2P trading
$P_{\omega,m,i,t}^{\text{SOP}}, Q_{\omega,m,i,t}^{\text{SOP}}$	Active/reactive power injected by $m$ -th SOP at node $i$ in period $t$ during scenario $\omega$
$P_{\omega,m,i,t}^{\text{SOP,L}}$	Active power loss of $m$ -th SOP connected to node $i$ in period $t$ during scenario $\omega$
$P_{\omega,i,t}^{\text{DG}}, Q_{\omega,i,t}^{\text{DG}}$	Active/reactive power injected by renewable DG at node $i$ in period $t$ during scenario $\omega$
$S_{\omega,m,k,t}^{\text{SOP}}$	Capacity usage of $m$ -th SOP connected to area $k$ in period $t$ during scenario $\omega$
$S_{k,m}^{\text{SOP}}$	Capacity of $m$ -th SOP planned by DISCO $k$
<b>Parameters</b>	
$N^{\text{TS}}, N^{\text{T}}$	Number of typical scenarios/time periods

$N_m^R$	Number of areas connected to $m$ -th SOP
$c^{AC}, c^L$	Per unit cost of converter/tie-line
$\Gamma_{\omega,t}^U$	Penalty price of voltage deviation in period $t$ during scenario $\omega$
$\pi_t^{G,buy}, \pi_t^{G,sell}$	Price of electricity purchased and sold to the upper grid in period $t$
$\pi_t^{P2P,max}$	Upper limit of P2P pricing in period $t$
$\Lambda^U, \Lambda^L$	Upper/lower boundary of master-problem
$\bar{V}, \underline{V}$	Upper/lower limit of square voltage
$r_{ij}, x_{ij}$	Resistance/reactance of line $ij$
$V_i^*$	Rated value of square voltage at node $i$
$A^{AC}$	Loss coefficient of converter

## I. INTRODUCTION

THE large-scale integration of distributed energy resources and charging loads poses significant challenges to the balance between power supply and demand in distribution networks (DNs) [1]. Limited by the acting frequency of the primary regulation equipment [2], conventional adjustment means have difficulties in responding to rapid fluctuations in power flows. This mismatch in time-scale has led to an increasing demand for flexible resources [3], which are highly effective in grid regulation [4]. Meanwhile, the novel power distribution devices based on power electronic technologies, represented by soft open points (SOPs), provide the fundamentals for the feasibility of flexible regulation [5]. By integrating the complementary benefits of multi-type resources in spatial and temporal aspects, the SOP is able to optimize power flows in real-time and improve the operation performance [6]. Thus, its role as an important flexible resource has been increasingly emphasized.

In recent years, the emergence of the local energy market [7] has driven a rise in peer-to-peer (P2P) electricity trading [8], creating a new demand for the application of SOPs [9]. To support the execution of P2P trading [10], it is required to integrate the complementary benefits of distributed sources [11] and loads [12]. Moreover, the introduction of a P2P market manager has been found in [13], [14] to be effective in privacy protection and social welfare improvement. With the ability to match the sources and loads for P2P trading, SOPs are well-suited for the organization and monitoring of trading activities among multi-stakeholders. The authors in [15] focused on flexible electricity trading and verified that P2P trading led by SOPs effectively reduced total operational costs. A game-based P2P trading method was further designed in [16] that enabled SOPs to generate self-revenue. However, given the substantial investment in SOPs, there is an urgent need for a sensible configuration of SOPs to help fully exploit their potential in the P2P market.

Previous studies focused on the optimal configuration of SOPs with the involvement of a single stakeholder [17], verifying the high return on investment of SOPs [18]. However, with the participation of new stakeholders in the local energy market, planning cannot be driven solely by the interests of a single stakeholder. The interests of different stakeholders may lead to operational results that differ from

those planned, raising a need to investigate the effect of SOP planning with multi-stakeholder participation. A coordinated planning method for renewable distributed generators (DGs) and SOPs under multi-stakeholder participation was presented in [19], which also helped the distribution company (DISCO) achieve higher returns by investing in SOPs.

Nevertheless, existing approaches mainly concern a single DISCO's investment in SOPs, ignoring the self-revenue of SOPs from P2P trading, which is attractive to all stakeholders. In a monopoly investment, the investor invests in a planning scheme that is best for him and ignores the claims of others. Such investments fall short of fully exploiting the mutual benefits of SOP integration. Besides, without considering the power fluctuation caused by P2P trading, the applicability of SOP planning may be affected. To fully benefit from the flexible resources [20] and alleviate the insufficient investment budget of some DISCOs [21], all stakeholders are allowed to invest jointly in SOPs driven by P2P trading.

With the development of power markets [22], different stakeholders emerge in DNs [23]. When multi-stakeholders are involved in the planning and investment of SOPs, conflicts arise because of the competition for resource allocation [24]. The varying interests of stakeholders drive the different planning and investment desires of SOPs. In competitive environments, game theory is effective in balancing the interests of multi-stakeholders [25]. Especially, cooperative games are often formed to maximize mutual benefits and generate higher returns for each stakeholder [26]. Besides, the inevitability of cooperation under joint investment has motivated the study of cooperative game planning for SOPs.

Focusing on the algorithms for solving cooperative game problems, two types have been identified, namely the centralized solution algorithm and the distributed solution algorithm [27]. Implementing a centralized solution algorithm requires a substantial amount of sensitive information from stakeholders, which is a challenge to obtain in practice. In contrast, the distributed solution algorithm, represented by ADMM [28], has been proved in [29] to be more applicable in resolving multi-stakeholder game problems. By minimizing variable interactions in ADMM, the sensitive privacy of multi-stakeholders can be effectively protected.

According to the forming mechanism of cooperation, cooperative games can be divided into coalition and Nash bargaining games [30]. For coalition games, the detection of stable coalitions requires the evaluation of all coalitions and their values, which significantly increases the computational complexity. By contrast, a Nash bargaining game model is more feasible when more stakeholders are involved [31].

In the standard bargaining game models, stakeholders are assumed to share the same benefits without differentiating their varying contributions, which may lead to conflicts in fair allocations. Such conflicts have created a market for the deployment of asymmetric bargaining games [32], which facilitate fair allocation by drawing on the created values of stakeholders [33]. Note that the desires of different stakeholders to invest and trade in the P2P market may differ,

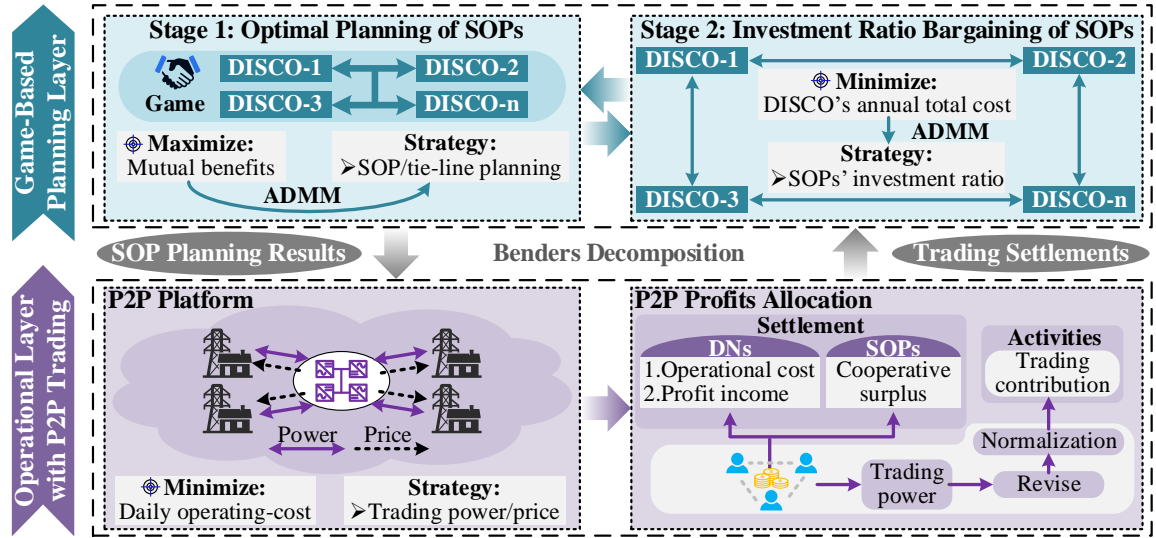


Fig. 1. Asymmetric bargaining-based planning framework for SOPs.

failing to consider these contributions together can result in an uneven resource allocation and affect cooperation. Therefore, driven by P2P electricity trading, an incentive-based allocation mechanism is required to encourage multi-stakeholder participation in game planning.

Aiming at the optimal SOP configuration under joint investment, an asymmetric bargaining-based planning method is proposed for SOPs considering P2P trading. By properly configuring the different capacities at multiple converters in SOP, the regulatory potential of SOP is fully explored and further increases the profits of stakeholders.

The major contributions are summarized as follows:

- 1) A planning-operation two-layer coupling framework is proposed under multi-stakeholder games. In the planning layer, the SOP planning scheme and its fair allocation among multi-stakeholders are determined based on the asymmetric bargaining. In the operational layer, the P2P trading and the profitability of multi-stakeholders are driven by price incentives.
- 2) An incentive-based allocation mechanism for the cooperative surplus is constructed by valuing each stakeholder's investment desire in SOPs and their corresponding contribution to P2P trading. The fair allocation encourages the joining of multi-stakeholders.
- 3) A three-step decomposition method is designed to solve the two-layer coupling model by combining the alternating direction multiplier method (ADMM) and generalized Benders decomposition (GBD) algorithm. To improve solution efficiency and accuracy, ADMM is modified with an update accelerated iteration strategy.

The remainder of this paper is organized as follows. Section II builds a planning-operation two-layer coupling framework of SOPs under multi-stakeholder games. In Section III, a game planning model for SOPs is established based on the asymmetric bargaining. The P2P energy trading-driven operational model of SOPs is given in Section IV. Section V describes the two-layer coupling model and the solution procedure. The case studies based on a practical case are given in Section VI and the conclusions are stated in Section VII.

## II. PLANNING-OPERATION TWO-LAYER COUPLING FRAMEWORK OF SOPs UNDER MULTI-STAKEHOLDER GAMES

In this study, it is assumed that each regional DN belongs to a different DISCO, with each DISCO considered as a stakeholder. By involving stakeholders in the joint investment and planning of SOPs, a game relation for resource allocation is considered among DISCOs. In addition, a planning-operation two-layer coupling framework of SOPs is designed, as shown in Fig. 1.

In the game-based planning layer, a fair profit-allocation mechanism is employed to encourage SOP investment among multiple DISCOs. Based on asymmetric bargaining, the game process among multiple DISCOs is decomposed into two stages that can be sequentially solved by ADMM. During the first stage, each DISCO pursues its interests and determines the planning scheme of SOPs and tie-lines. In the second stage, multiple DISCOs compete for a cooperative surplus by utilizing their bargaining power (BP). During competition at this stage, the ratio of each stakeholder in the SOP investment is determined. To fully motivate the joining of DISCOs, the BP is decided by considering each DISCO's investment desire in SOPs and their corresponding contribution to P2P trading.

In the operational layer, a non-profit SOP operator is introduced to facilitate P2P trading among multiple DISCOs and prevent them from gathering sensitive operating data from each other. In the P2P trading, the SOP operator sets P2P prices based on the ratio of power supply to demand reported by each area. Driven by price incentives, DISCOs participate in P2P trading to increase profits. During this process, the heavily loaded DISCOs urgently require power injections to alleviate the power shortage, thereby accepting the high P2P prices. While DISCOs with high renewable DG penetration are willing to provide power at a lower pricing to reduce DG shedding. The cost differences that arise from P2P trading with different areas are collected by the SOP operator and then shared among DISCOs as a cooperative surplus. During the P2P process, the SOP operator does not benefit from the organization of trading, making it a non-profit SOP operator.

Due to the dual-layer structure of the framework, it is difficult to be solved directly. Besides, it is required to protect the sensitive scheduling information of different DISCOs in the competition. Thus, the GBD algorithm is applied to realize parameter transfer between the two layers. The planning strategies act as preconditions for the operational layer. Meanwhile, trading results in the lower layer provide information to facilitate decision-making in the planning layer.

### III. GAME PLANNING MODEL OF SOPs WITH MULTI-STAKEHOLDER JOINT INVESTMENT

In this section, game behavior analysis is conducted based on the interests of multi-stakeholders. Subsequently, an SOP bargaining-based planning model is established, which is decomposed into two stages, the optimal planning and the investment ratio bargaining of SOPs. To improve solution efficiency and accuracy, the ADMM algorithm is modified with an update accelerated iteration strategy.

#### A. Analysis on Game Behavior of Multi-Stakeholders

Aiming to minimize its annual total costs, each DISCO determines the planning schemes and investment strategies of SOPs independently. Areas that operate with heavy loads or highly penetrated DGs would invest in large-capacity SOPs to transfer electricity. Conversely, areas with a better balance between power demand and supply may not be willing to support the planning and investment of large-capacity SOPs. Given the varying power demands of different stakeholders, there arise conflicts in the planning and investment of SOPs.

Therefore, it is evident that different DISCOs influence each other when formulating planning and investment strategies, and forming a game problem, as shown in Fig. 2. Given the mutual benefits of DISCOs, it is crucial to establish a cooperative game model with a fair allocation mechanism.

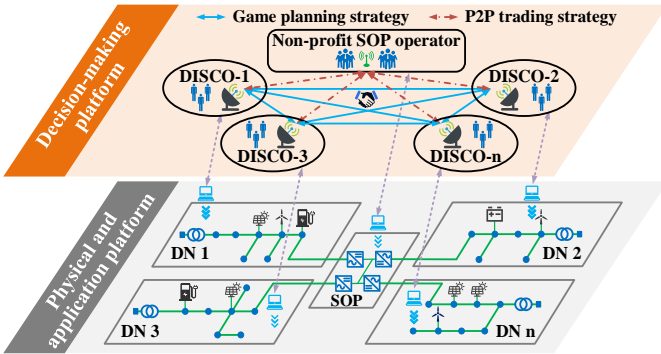


Fig. 2. Stakeholders of SOP planning and operation in DNs.

As can be observed from Fig. 2, the planning and investment strategies of SOPs are exchanged among DISCOs during the bargaining process. Besides, the P2P trading strategies need to be exchanged between the SOP operator and DISCOs. During the P2P trading, the SOP operator provides P2P prices, while DISCOs must respond with the active and reactive power that is expected to be traded.

#### B. Game Planning Model of SOPs

In the SOP planning process, the DISCOs pursue their own goals and make decisions independently. Thus, the benefits

and costs model for each DISCO is established separately to construct an SOP bargaining-based planning model.

#### 1) Benefits and costs of regional DISCO

The objective of each DISCO is to minimize the annual total cost  $F_k^{\text{DN}}$ , as illustrated in (1).

$$F_k^{\text{DN}} = \min(-R_k^{\text{P}} + C_k^{\text{I}} + C_k^{\text{Line}} + C_k^{\text{S}} + C_k^{\text{O}} + C_k^{\text{G}} + C_k^{\text{P2P}} + C_k^{\text{U}}) \quad (1)$$

##### • Annual sharing of cooperative surplus

Based on price incentives, the SOP operator acquires electricity at a low payment and then sends it to areas with demand at a high price. This process creates a cooperative surplus by collecting cost differences, as indicated in (2.a) and (2.b). Then, according to the investment ratios of each DISCO, the cooperative surplus is allocated, as given in (2.c).

$$R_m^{\text{P}} = 365 \sum_{\omega=1}^{N^{\text{TS}}} \sum_{t=1}^{N^{\text{T}}} f_{\omega,m,t}^{\text{P}} p_{\omega} \quad (2.a)$$

$$f_{\omega,m,t}^{\text{P}} = \sum_{k \in \Omega^{\text{R}}} (\pi_{\omega,k,t}^{\text{P}} P_{\omega,m,k,t}^{\text{SOP}} + \pi_{\omega,k,t}^{\text{Q}} Q_{\omega,m,k,t}^{\text{SOP}}) \quad (2.b)$$

$$R_k^{\text{P}} = \sum_{m \in \Omega_k^{\text{SOP}}} \mu_{m,k} R_m^{\text{P}} \quad (2.c)$$

where  $f_{\omega,m,t}^{\text{P}}$  is the cooperative surplus from the  $m$ -th SOP in period  $t$  during scenario  $\omega$ .

##### • Annual investment cost in SOPs

Considering the discount rate  $d$  and device lifetime  $y$ , the SOP investment cost of DISCO  $k$  is shown as follows.

$$C_k^{\text{I}} = \sum_{m \in \Omega_k^{\text{SOP}}} \mu_{m,k} C_m^{\text{SOP}} \quad (3.a)$$

$$C_m^{\text{SOP}} = \sum_{i \in \Omega_m^{\text{AC}}} \frac{d(1+d)^y}{(1+d)^y - 1} C_{S_{m,i}}^{\text{AC}} \quad (3.b)$$

##### • Annual investment cost of tie-lines

The investment of tie-lines is completed by the DISCO directly connected to it, resulting in the follows.

$$C_k^{\text{Line}} = \sum_{ij \in \Omega_k^{\text{SOP,Line}}} \frac{d(1+d)^y}{(1+d)^y - 1} \psi c^{\text{L}} l_{ij} \quad (4)$$

where  $l_{ij}$  denotes the length of the planned line  $ij$ .  $\psi$  is the terrain correction coefficient.

##### • Annual investment cost of land expropriation

Considering the land expropriation price  $c_m^{\text{site}}$ , the annual investment cost of land is given in (5).

$$C_k^{\text{S}} = \sum_{m \in \Omega_k^{\text{SOP}}} \frac{d(1+d)^y}{(1+d)^y - 1} \mu_{m,k} c_m^{\text{site}} \quad (5)$$

##### • Annual cost of SOP maintaining

Introducing the factor of maintaining  $\eta$ , the annual maintenance cost of SOPs can be calculated as follows.

$$C_k^{\text{O}} = \sum_{m \in \Omega_k^{\text{SOP}}} \mu_{m,k} C_m^{\text{SOP,O}} \quad (6.a)$$

$$C_m^{\text{SOP,O}} = \eta \sum_{i \in \Omega_m^{\text{AC}}} C_{S_{m,i}}^{\text{AC}} \quad (6.b)$$

##### • Annual purchase cost from upper grid

As each area trades only as a buyer or seller with the upper grid, only one of  $P_{\omega,k,t}^{\text{S,g}}$  or  $P_{\omega,k,t}^{\text{B,g}}$  can exist. To better model the actual operation of DNs, a distinction is made between the prices of electricity purchased and sold to the upper grid, as given in (7).

$$C_k^{\text{G}} = 365 \sum_{\omega=1}^{N^{\text{TS}}} \sum_{t=1}^{N^{\text{T}}} f_{\omega,k,t}^{\text{G}} p_{\omega} \quad (7.a)$$

$$f_{\omega,k,t}^{\text{G}} = \pi_t^{\text{G,buy}} P_{\omega,k,t}^{\text{B,g}} - \pi_t^{\text{G,sell}} P_{\omega,k,t}^{\text{S,g}} \quad (7.b)$$

where  $f_{\omega,k,t}^G$  presents the purchase cost from the upper grid of area  $k$  in period  $t$  during scenario  $\omega$ .

- *Annual purchase cost in P2P trading*

The annual payment cost incurred by DISCO  $k$  in the P2P market is depicted in (8).

$$C_k^{P2P} = 365 \sum_{\omega=1}^{N^{TS}} \sum_{t=1}^{N^T} f_{\omega,k,t}^{P2P} p_{\omega} \quad (8.a)$$

$$f_{\omega,k,t}^{P2P} = \sum_{i \in \Omega_k^{SOP}} (\pi_{\omega,k,t}^P P_{\omega,i,t}^{SOP} + \pi_{\omega,k,t}^Q Q_{\omega,i,t}^{SOP}) \quad (8.b)$$

- *Annual cost of voltage deviation*

Based on the voltage deviation ratio and the cost of non-serve energy in extreme situations, the voltage deviation term is formulated in (9).

$$C_k^U = 365 \sum_{\omega=1}^{N^{TS}} \sum_{t=1}^{N^T} f_{\omega,k,t}^U p_{\omega} \quad (9.a)$$

$$f_{\omega,k,t}^U = \sum_{i \in \Omega_k^N} \Gamma_{\omega,t}^U P_{\omega,i,t}^{LD} V_{\omega,i,t}^{dev} \quad (9.b)$$

where  $f_{\omega,k,t}^U$  is the voltage deviation cost of area  $k$  in period  $t$  during scenario  $\omega$ .

To improve solving efficiency, the indicator of voltage deviation is linearized in segments and then relaxed in (10). Besides, the linearization result of the voltage deviation term is presented in Fig. 3.

$$V_{\omega,i,t}^{dev} \geq \frac{V_{thr} - V_{\omega,i,t}}{V_{thr} - \bar{V}}, i \in \Omega_k^N \quad (10.a)$$

$$V_{\omega,i,t}^{dev} \geq 0, i \in \Omega_k^N \quad (10.b)$$

$$V_{\omega,i,t}^{dev} \geq \frac{V_{\omega,i,t} - \bar{V}_{thr}}{\bar{V} - \bar{V}_{thr}}, i \in \Omega_k^N \quad (10.c)$$

where  $\underline{V}_{thr}$  and  $\bar{V}_{thr}$  are the lower and upper limits of desired voltage interval, respectively.

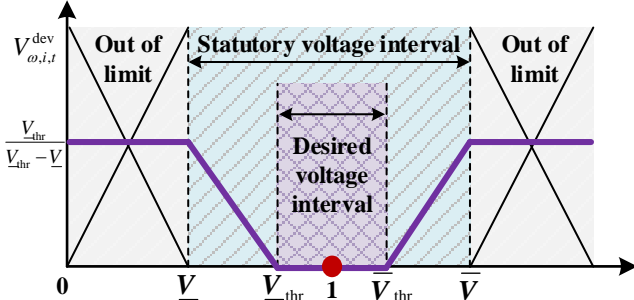


Fig. 3. Linearization result of voltage deviation term.

Additionally, the SOP investment ratio among multiple DISCOs must satisfy the following constraints.

$$\sum_{k \in \Omega^R} \mu_{m,k} = 1, m \in \Omega^{SOP} \quad (11)$$

When the  $m$ -th SOP is not physically connected to area  $k$ , DISCO  $k$  is precluded from investing in that SOP, as indicated by  $\mu_{m,k}$  being set to zero.

## 2) Asymmetric bargaining-based planning for SOPs

To facilitate fair allocation, the BP of DISCOs, denoted as  $\tau_k$ , is introduced to construct an asymmetric bargaining model, as built in (12). Unlike the standard bargaining model where the BP is ignored, an asymmetric BP in (12) is designed to show the importance of each stakeholder in cooperation.

$$F = \max \prod_{k \in \Omega^R} [F_k^{DN,0} - F_k^{DN}]^{\tau_k} \quad (12.a)$$

$$\text{s.t.} \begin{cases} (10), (11) \\ F_k^{DN} \leq F_k^{DN,0}, k \in \Omega^R \end{cases} \quad (12.b)$$

where  $F_k^{DN,0}$  denotes the total cost of DISCO  $k$  during the independent operations.

Model (12) is non-convex and nonlinear, which makes it difficult to solve directly. Consequently, the original problem is transformed into a two-stage problem as follows.

### Stage 1: Maximizing mutual benefits

For multi-stakeholders, solving the problem of maximizing mutual benefits is equivalent to minimizing costs. Briefly, the model for **Stage 1** can be described as follows:

$$F^{S1} = \min(\sum_{k \in \Omega^R} F_k^{DN}) \quad (13.a)$$

$$\text{s.t.} \begin{cases} (10), (11) \\ F_k^{DN} \leq F_k^{DN,0}, k \in \Omega^R \end{cases} \quad (13.b)$$

### Stage 2: Bargaining of SOP investment ratios

To make a fair allocation of cooperative surplus among DISCOs, it is crucial to quantify the BP of each stakeholder.

Firstly, based on the amount of P2P power, an exponential model is applied to quantify trading contribution  $g_{m,k}$  in (14).

$$E_{m,k}^B = \sum_{\omega=1}^{N^{TS}} \sum_{t=1}^{N^T} E_{\omega,m,k,t}^{SOP} p_{\omega}, P_{\omega,m,k,t}^{SOP} \geq 0 \quad (14.a)$$

$$E_{m,k}^S = \sum_{\omega=1}^{N^{TS}} \sum_{t=1}^{N^T} E_{\omega,m,k,t}^{SOP} p_{\omega}, P_{\omega,m,k,t}^{SOP} < 0 \quad (14.b)$$

$$E_{\omega,m,k,t}^{SOP} = \sqrt{(P_{\omega,m,k,t}^{SOP})^2 + (Q_{\omega,m,k,t}^{SOP})^2} \quad (14.c)$$

$$g_{m,k} = e^{\frac{E_{m,k}^S}{\max(E_{m,1}^S, \dots, E_{m,k}^S)}} - e^{\frac{-E_{m,k}^B}{\max(E_{m,1}^B, \dots, E_{m,k}^B)}} \quad (14.d)$$

where  $E_{\omega,m,k,t}^{SOP}$  is the capacity usage of  $m$ -th SOP by DISCO  $k$  in period  $t$  during scenario  $\omega$ .

Given the high cost of SOP losses, the BP should be revised to encourage investment, which results in the calculation of the revision factor  $\psi_{m,k}$  as follows.

$$E_{m,k}^L = \sum_{\omega=1}^{N^{TS}} \sum_{t=1}^{N^T} \sum_{i \in \Omega_k^{SOP}} \max(P_{\omega,i,t}^{SOP,L}, 0) p_{\omega} \quad (15.a)$$

$$\psi_{m,k} = e^{\frac{E_{m,k}^L}{\max(E_{m,1}^L, \dots, E_{m,k}^L)}} - e^{\frac{-E_{m,k}^B}{\max(E_{m,1}^B, \dots, E_{m,k}^B)}} \quad (15.b)$$

Furthermore, the P2P trading contributions of each DISCO are normalized in (16).

$$D_{m,k} = \frac{(g_{m,k} - \psi_{m,k})}{\sum_{r \in \Omega^R} (g_{m,r} - \psi_{m,r})} \quad (16)$$

Finally, based on the investment ratios of multiple DISCOs, the BP can be determined in (17).

$$\tau_k = \sum_{m \in \Omega_k^{SOP}} \tau_{m,k} = \sum_{m \in \Omega_k^{SOP}} \frac{(D_{m,k} + \mu_{m,k})}{2} \quad (17)$$

where  $\tau_{m,k}$  corresponds to the BP of DISCO  $k$  when investing in the  $m$ -th SOP.

By converting model (12) into logarithmic form and incorporating (14)-(17), the complete model for **Stage 2** is then illustrated as follows.

$$F^{S2} = \max(\sum_{k \in \Omega^R} \tau_k \ln(F_k^{DN,0} - F_k^{DN})) \quad (18.a)$$

$$\text{s.t.} \begin{cases} (14) - (17) \\ F_k^{DN} \leq F_k^{DN,0}, k \in \Omega^R \end{cases} \quad (18.b)$$

In particular,  $f_k^{DN}$  in **Stage 2** is shown as follows.

$$f_k^{DN} = -R_k^P + C_k^I + C_k^{\text{Line},*} + C_k^S + C_k^O + C_k^{G,*} + C_k^{P2P,*} + C_k^{U,*} \quad (19)$$

where the variable marked with “\*” denotes the optimal solution of **Stage 1**, and similarly in the rest.

### C. Solving Method Based on ADMM

Given the requirements for both fast and precise solutions to large-scale problems, the ADMM is adopted to design bargaining strategies in the planning layer. Simultaneously, by minimizing variable interactions in ADMM, the private dispatch information of multiple DISCOs is protected.

#### 1) Solution for optimal siting and sizing of SOPs

Firstly, to determine the optimal SOP planning scheme, the auxiliary variable  $\hat{S}_{k,m}^{\text{SOP}}$  is introduced.

$$\hat{S}_{k,m}^{\text{SOP}} = \frac{1}{N_m^R - 1} \sum_{r \in \Omega_m^R, r \neq k} S_{r,m}^{\text{SOP}}, m \in \Omega_k^{\text{SOP}}, k \in \Omega^R \quad (20)$$

When  $S_{k,m}^{\text{SOP}} = \hat{S}_{k,m}^{\text{SOP}}, m \in \Omega_k^{\text{SOP}}, k \in \Omega^R$  is satisfied, it indicates that a consensus on SOP planning has been reached.

Subsequently, the Lagrangian multiplier  $\lambda_{k,m}^{\text{CAP}}$  with the penalty parameter  $\rho$  is introduced to form the augmented Lagrangian function (21).

$$L^{S1} = \min \left( F^{S1} + \sum_{k \in \Omega^R} \sum_{m \in \Omega_k^{\text{SOP}}} \left( \lambda_{k,m}^{\text{CAP}} (S_{k,m}^{\text{SOP}} - \hat{S}_{k,m}^{\text{SOP}}) + \frac{\rho}{2} \|S_{k,m}^{\text{SOP}} - \hat{S}_{k,m}^{\text{SOP}}\|_2^2 \right) \right) \quad (21)$$

As shown in (22), (21) is decomposed into the ADMM jointly-based distributed optimization problems. Note that only  $S_{k,m}^{\text{SOP}}$  needs to be exchanged among DISCOs, which enables the protection of sensitive scheduling information.

The planning objective function for each DISCO is expressed as follows.

$$L_k^{S1} = \min \left( F_k^{\text{DN}} + \sum_{m \in \Omega_k^{\text{SOP}}} \left( \lambda_{k,m}^{\text{CAP}} (S_{k,m}^{\text{SOP}} - \hat{S}_{k,m}^{\text{SOP}}) + \frac{\rho}{2} \|S_{k,m}^{\text{SOP}} - \hat{S}_{k,m}^{\text{SOP}}\|_2^2 \right) \right) \quad (22)$$

Additionally, at iteration  $Z$ , the Lagrangian multipliers for  $m$ -th SOP of **Stage 1** are updated according to (23).

$$\lambda_{k,m}^{\text{CAP}}(Z+1) = \lambda_{k,m}^{\text{CAP}}(Z) + \rho (S_{k,m}^{\text{SOP}}(Z) - \hat{S}_{k,m}^{\text{SOP}}(Z)) \quad (23)$$

Finally, the details of the ADMM-based distributed solution process are expressed in Appendix A.

#### 2) Solution for investment ratio bargaining of SOPs

To determine the optimal investment ratios of DISCOs, the auxiliary variable  $\hat{\mu}_{m,k}$  is introduced in (24).

$$\hat{\mu}_{m,k} = 1 - \sum_{r \in \Omega^R, r \neq k} \mu_{m,r}, m \in \Omega_k^{\text{SOP}}, k \in \Omega^R \quad (24)$$

By adding the Lagrangian multiplier  $\lambda_{m,k}^{\text{DN}}$ , the augmented Lagrangian function for **Stage 2** is established in (25).

$$L^{S2} = \min \left( -F^{S2} + \sum_{k \in \Omega^R} \left( \sum_{m \in \Omega_k^{\text{SOP}}} \tau_{m,k} \lambda_{m,k}^{\text{DN}} (\mu_{m,k} - \hat{\mu}_{m,k}) + \frac{\rho}{2} \sum_{k \in \Omega^R} \sum_{m \in \Omega_k^{\text{SOP}}} \|\mu_{m,k} - \hat{\mu}_{m,k}\|_2^2 \right) \right) \quad (25)$$

Moreover, to determine the optimal investment ratio among  $N^R$  DISCOs, (25) is decomposed into multiple independent investment payment objective functions, as given in (26).

$$L_k^{S2} = \min \left( -\tau_k \ln(F_k^{\text{DN},0} - f_k^{\text{DN}}) + \sum_{m \in \Omega_k^{\text{SOP}}} \left( \tau_{m,k} \lambda_{m,k}^{\text{DN}} (\mu_{m,k} - \hat{\mu}_{m,k}) + \frac{\rho}{2} \|\mu_{m,k} - \hat{\mu}_{m,k}\|_2^2 \right) \right) \quad (26)$$

Finally, an expatriation of the ADMM-based distributed solution process is utilized to solve (26). On this basis, details

are shown as provided in Appendix A, and the Lagrangian multipliers of **Stage 2** are updated according to (27).

$$\lambda_{m,k}^{\text{DN}}(Z+1) = \lambda_{m,k}^{\text{DN}}(Z) + \rho (\mu_{m,k}(Z) - \hat{\mu}_{m,k}(Z)) \quad (27)$$

## IV. P2P TRADING-DRIVEN OPERATIONAL MODEL OF SOPs

To further improve the operational status of DNs, the P2P trading is introduced as an auxiliary trading form that can complement the trading with upper grid. The demand for P2P trading is driven by power imbalances between different areas. Therefore, it is necessary to quantify the power demand of each area to determine the dispatch price.

Firstly, a predicted ratio of renewable DG output to load demand is supplied by each DISCO, as given in (28.a). Next, based on the power supply to demand ratio offered by DISCOs, the SOP operator determines the active P2P prices [34] as indicated in (28.b). Additionally, the prices for reactive auxiliary services [35] are shown in (28.c).

$$\varpi_{\omega,k,t} = \frac{\sum_{i \in \Omega_k^N} P_{\omega,i,t}^{\text{DG}}}{\sum_{i \in \Omega_k^N} P_{\omega,i,t}} \quad (28.a)$$

$$\pi_{\omega,k,t}^P = \max \left\{ \frac{\pi_t^{\text{G,sell}} \pi_t^{\text{G,buy}}}{(\pi_t^{\text{G,buy}} - \pi_t^{\text{G,sell}}) \varpi_{\omega,k,t} + \pi_t^{\text{G,sell}}}, \pi_t^{\text{G,sell}} \right\} \quad (28.b)$$

$$\pi_{\omega,k,t}^Q = 0.2 \pi_{\omega,k,t}^P \quad (28.c)$$

As can be seen from (28.b), the prices for P2P active power are maintained within the range of purchasing and selling prices with the upper grid. This results in greater profitability for DISCOs to actively participate in P2P trading. Besides, the trading activities should satisfy the following constraints.

$$\sum_{k \in \Omega_m^{\text{AC}}} (\pi_{\omega,k,t}^P P_{\omega,m,k,t}^{\text{SOP}}) \geq 0, m \in \Omega^{\text{SOP}} \quad (29.a)$$

$$\sum_{k \in \Omega_m^{\text{AC}}} (\pi_{\omega,k,t}^Q Q_{\omega,m,k,t}^{\text{SOP}}) \geq 0, m \in \Omega^{\text{SOP}} \quad (29.b)$$

To enhance mutual benefits, an objective function in the operational layer is established by the SOP operator. Specifically, the daily operating costs of each DISCO are integrated, as expressed in (30).

$$f_{\omega,t}^{\text{OP}} = \min (\sum_{k \in \Omega^R} (f_{\omega,k,t}^{\text{G}} + f_{\omega,k,t}^{\text{P2P}} + f_{\omega,k,t}^{\text{U}})) \quad (30)$$

The operational constraints of  $m$ -th SOP are shown in (31).

$$\sum_{i \in \Omega_m^{\text{AC}}} P_{\omega,m,i,t}^{\text{SOP}} - \sum_{i \in \Omega_m^{\text{AC}}} P_{\omega,m,i,t}^{\text{SOP,L}} = 0 \quad (31.a)$$

$$P_{\omega,m,i,t}^{\text{SOP,L}} = \text{AC} \sqrt{(P_{\omega,m,i,t}^{\text{SOP}})^2 + (Q_{\omega,m,i,t}^{\text{SOP}})^2} \quad (31.b)$$

$$\sqrt{(P_{\omega,m,i,t}^{\text{SOP}})^2 + (Q_{\omega,m,i,t}^{\text{SOP}})^2} \leq S_{m,i}^{\text{SOP}} \quad (31.c)$$

The operational constraints of DN are illustrated as follows.

$$\sum_{ki \in \Omega_k^+} (P_{\omega,ki,t} - r_{ki} I_{\omega,ki,t}) + P_{\omega,i,t} = \sum_{ij \in \Omega_k^+} P_{\omega,ij,t} \quad (32.a)$$

$$\sum_{ki \in \Omega_k^+} (Q_{\omega,ki,t} - x_{ki} I_{\omega,ki,t}) + Q_{\omega,i,t} = \sum_{ij \in \Omega_k^+} Q_{\omega,ij,t} \quad (32.b)$$

$$P_{\omega,i,t} = P_{\omega,i,t}^{\text{DG}} + P_{\omega,i,t}^{\text{SOP}} - P_{\omega,i,t}^{\text{LD}}, i \in \Omega_k^N \quad (32.c)$$

$$Q_{\omega,i,t} = Q_{\omega,i,t}^{\text{DG}} + Q_{\omega,i,t}^{\text{SOP}} - Q_{\omega,i,t}^{\text{LD}}, i \in \Omega_k^N \quad (32.d)$$

$$V_{\omega,i,t} - V_{\omega,j,t} + (r_{ij}^2 + x_{ij}^2) I_{\omega,ij,t} = 2(r_{ij} P_{\omega,ij,t} + x_{ij} Q_{\omega,ij,t}) \quad (32.e)$$

$$I_{\omega,ij,t} V_{\omega,i,t} = P_{\omega,ij,t}^2 + Q_{\omega,ij,t}^2 \quad (32.f)$$

Eqs. (32.a) and (32.b) include the nodal active and reactive power injection constraints, respectively. Eq. (32.e) expresses

the voltage drop of line  $ij$ . Besides, the details of the operational layer are addressed as [5].

### V. PLANNING-OPERATION TWO-LAYER COUPLING MODEL OF SOPs

In this section, a planning-operation two-layer coupling model of SOPs is developed. To realize parameter transfer between the two layers and protect the sensitive dispatching information, the GBD algorithm is introduced. Subsequently, by combining the ADMM and GBD algorithms, a complete solution procedure for the two-layer model is established.

#### A. Two-Layer Model Based on GBD

The two-layer coupling model based on the asymmetric bargaining is summarized in (33).

$$\max F \quad (33.a)$$

$$\text{s.t.} \begin{cases} (10), (11), (14) - (17), (28), (29), (31), (32) \\ F_k^{\text{DN}} \leq F_k^{\text{DN},0}, k \in \Omega^{\text{R}} \end{cases} \quad (33.b)$$

To determine SOP planning schemes in the planning layer, it is essential to collect operational information such as P2P results from lower layer. Thus, the GBD algorithm is adopted in this study. By adding Benders cuts to the master-problem (MP), parameters can be transferred between the two layers without revealing any sensitive dispatching data of DNs.

Firstly, by considering the operational layer, the model of the first stage can be reformed in (34). It is then divided into an MP and multiple independent scenario-based operational sub-problems (SPs).

$$\min F^{\text{S1}} \quad (34.a)$$

$$\text{s.t.} \begin{cases} (10), (11), (28), (29), (31), (32) \\ F_k^{\text{DN}} \leq F_k^{\text{DN},0}, k \in \Omega^{\text{R}} \end{cases} \quad (34.b)$$

a) The aim of MP is to decide the planning scheme of SOPs and tie-lines, which is expressed as follows:

$$\min F^{\text{MP}} = a^{\text{T}}x + \sum_{\omega=1}^{N^{\text{TS}}} \Lambda_{\omega} p_{\omega} = \sum_{k \in \Omega^{\text{R}}} (C_k^{\text{I}} + C_k^{\text{Line}} + C_k^{\text{S}} + C_k^{\text{O}}) + \sum_{\omega=1}^{N^{\text{TS}}} \Lambda_{\omega} p_{\omega} \quad (35.a)$$

$$\text{s.t. } x \leq S^{\text{SOP,max}} \quad (35.b)$$

where  $a$  corresponds to the coefficient vectors in function  $\sum_{k \in \Omega^{\text{R}}} (C_k^{\text{I}} + C_k^{\text{Line}} + C_k^{\text{S}} + C_k^{\text{O}})$ .  $[\ ]^{\text{T}}$  represents the transposed

form of the matrix  $[\ ]$ .  $x$  denotes the set of decision variables for MP, including planning schemes of SOPs and tie-lines.  $\Lambda_{\omega}$  means an auxiliary variable that indicates lower bounds of the objective function in SP during scenario  $\omega$ .  $S^{\text{SOP,max}}$  is the upper installation limit of SOP capacity.

b) The objective of SP is to achieve optimal operation during each scenario, which is formulated in (36).

$$\min F_{\omega}^{\text{SP}} = \sum_{t \in N^{\text{T}}} f_{\omega,t}^{\text{OP}} \quad (36.a)$$

$$\text{s.t. } \|D_{\omega,n} y_{\omega}\| \leq j_{\omega,n} y_{\omega} + g_{\omega,n} \hat{x} : (\sigma_{\omega,n}, \tau_{\omega,n}), n = 1, \dots, N_1 \quad (36.b)$$

$$\|W_{\omega,n} y_{\omega}\| = w_{\omega,n} y_{\omega} : o_{\omega,n}, n = 1, \dots, N_2 \quad (36.c)$$

$$H_{\omega,n} y_{\omega} \leq h_{\omega,n} : \zeta_{\omega,n}, n = 1, \dots, N_3 \quad (36.d)$$

where  $\hat{x}$  is the decision variables translated from MP.  $y_{\omega}$  is the set of decision variables for the SP during scenario  $\omega$ , including renewable DG output, P2P prices, and power flows.

When  $\hat{x}$  is considered in the SP, the first constraint in (36) is formed to represent (31.c). In (36.b),  $D_{\omega,n}$  represents the coefficient matrix,  $j_{\omega,n}$  and  $g_{\omega,n}$  correspond to the constant vectors,  $\sigma_{\omega,n}$  and  $\tau_{\omega,n}$  are the dual multiplier vectors.  $N_1$  denotes the number of constraints contained in (36.b).

Without considering  $\hat{x}$ , the following constraints are obtained. In (36), the second constraint consists of (31.b), (32.e) and (32.f), while the last stands for (10), (28), (31.a) and (32.a)-(32.d). In (36.c),  $o_{\omega,n}$  represents the dual multiplier vector,  $W_{\omega,n}$  and  $w_{\omega,n}$  are the coefficient matrix and constant vector, respectively. In (36.d),  $\zeta_{\omega,n}$  is the dual multiplier vector,  $H_{\omega,n}$  and  $h_{\omega,n}$  denote the coefficient matrix and constant vector, respectively.  $N_2$  and  $N_3$  are the number of constraints contained in (36.c) and (36.d), respectively.

Finally, the planning scheme of different DISCOs can be determined by sequentially solving the MP and SPs, and the iterations are illustrated in Appendix B.

#### B. Solution Procedure

A method for solving the two-layer coupling model is proposed by combining ADMM and GBD algorithms. The solution procedure is described as follows:

As can be observed in Fig.4, after initialization, the

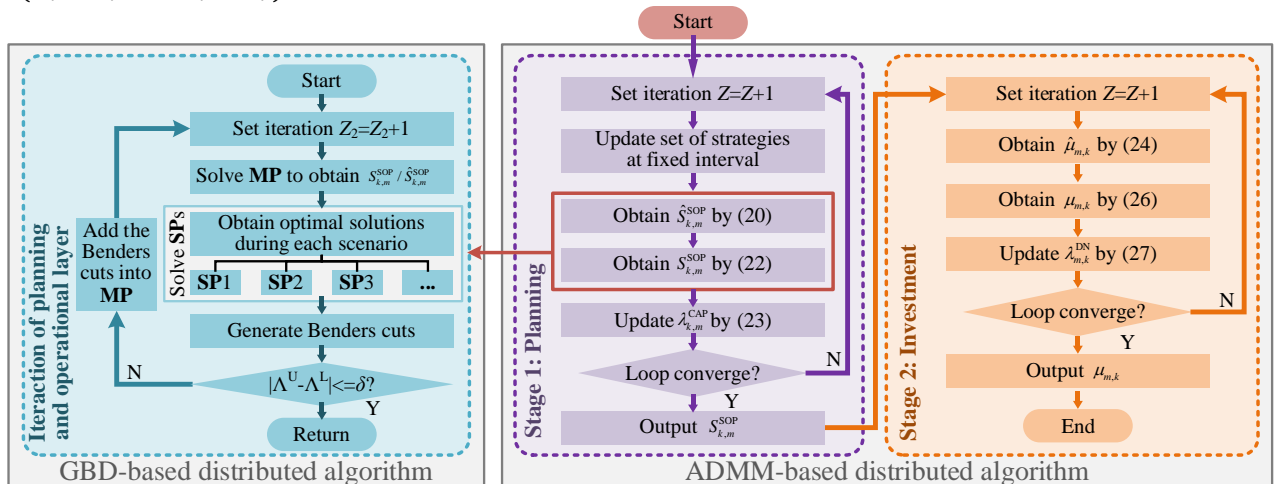


Fig. 4. Three-step decomposition method for the two-layer coupling model.



bargaining process of **Stage 1** starts. At the  $Z$ th iteration, with the objective of reducing the annual total costs, DISCO  $k$  adjusts its planning scheme based on the latest decisions of the other DISCOs. To determine the optimal planning scheme of SOPs and tie-lines, the GBD is employed to acquire P2P information in the planning layer. Then, the planning scheme of DISCO  $k$  is sent to the other DISCOs, and the other DISCOs determine their planning scheme following the same process. Finally, judge whether the game is in equilibrium at the  $Z$ th iteration. If not, move on to the next iteration.

If none of the DISCOs is able to increase profits through strategy adjustment, the game is balanced, as detailed in (37).

$$\widetilde{M}_k^D = \operatorname{argmax} F_k^G(M_k^D, \widetilde{M}_r^D), r \in \Omega^R, r \neq k \quad (37)$$

where  $M_k^D$  is the game strategy of DISCO  $k$ .  $F_k^G$  denotes the objective functions of DISCO  $k$ .  $\widetilde{M}_k^D$  is the optimal response of DISCO  $k$  when the strategy is given by the other DISCOs.

Once the planning scheme of SOPs has been determined, the bargaining process of **Stage 2** begins. In **Stage 2**, the optimal investment ratios of each DISCO are decided in turn. The bargaining process of **Stage 2** is similar to that of **Stage 1** and the details have not been repeated here. When the game of **Stage 2** is equilibrated, the optimal configuration of SOPs and their fair allocation among DISCOs are obtained. Besides, the proof of the optimality property is given in Appendix C.

In summary, the two-layer coupling model can be effectively solved by using available optimization packages.

## VI. CASE STUDIES AND ANALYSIS

In this section, the effectiveness of the proposed asymmetric bargaining-based planning method is verified on a modified practical distribution network in China. The proposed method is implemented in MATLAB R2016a. Numerical experiments are performed using CPLEX 12.8 solver in YALMIP on an Intel Core i7 @ 2.90GHz PC with 24GB RAM.

### A. Practical Distribution Networks

As demonstrated in Fig. 5, the system consists of two commercial areas and one residential area, of which the rated voltage level is 10.50 kV. The residential area has heavy loads, while commercial areas are opposite. The total active and reactive power demands are 20.744 MW and 6.587 MVar, respectively.

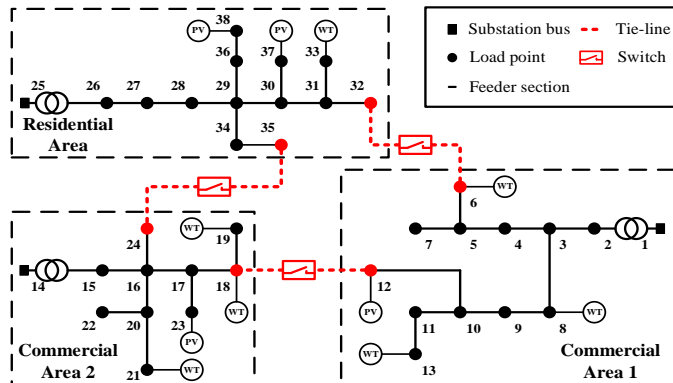


Fig. 5. Structure of the modified practical DNs in China.

For commercial areas, the active power of the renewable DG output reaches almost 100% of peak demand. In the residential area, the renewable DG penetration rate is close to 50%. The power factor of renewable DGs is assumed to be 0.9 and the parameters are listed in TABLE I. There are six nodes connected to tie-switches, and these are marked as red points in Fig. 5. The minimum and maximum statutory voltages are set to 0.90 p.u. and 1.10 p.u., respectively [3]. The upper and lower limits of desired voltage interval are set as [0.99, 1.01]. The time-of-use power price set by the upper grid is given in Fig. 6, and the trading period is set to 24 hours [13]. The voltage deviation penalty parameter  $\Gamma_{\omega,t}^U$  is set as  $\pi_t^G$ . The variation of SOP planning parameters is given in Table II [19].

TABLE I  
INSTALLATION PARAMETERS OF RENEWABLE DGs

Location	Capacity (kVA)	Type	Location	Capacity (kVA)	Type
6	2000	WT	28	2000	WT
8	1500	WT	211	1000	PV
12	1000	PV	39	1500	WT
13	1500	WT	313	1000	PV
25	2000	WT	314	1000	PV
26	2000	WT	-	-	-

TABLE II  
BASIC PLANNING PARAMETERS OF SOPs

Parameters	Value	Parameters	Value
AC-DC converter price $c^{AC}$ (CNY/kVA)	1000	Device lifetime $y$ (Year)	20
Line constructing price $c^L$ (CNY/km)	$10^4$	Discount rate $d$	0.08
Land expropriation price $c_m^{\text{site}}$ (CNY/Converter)	$10^6$	SOP maintaining factor $\eta$	0.01

By clustering the renewable DG output curve and load curve in a year, four typical scenarios in Fig. 7 are obtained, including the changes of loads, PV, and WT output in one day [36]. The probability values of the four typical scenarios are {0.2438, 0.2027, 0.3480, 0.2055}.

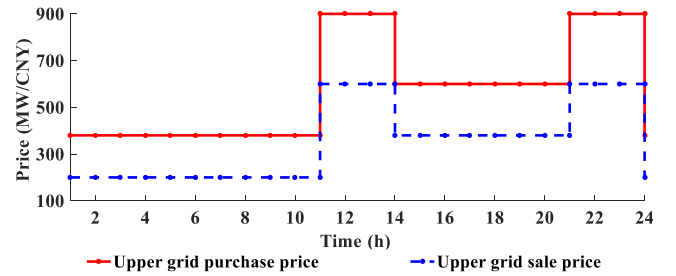


Fig. 6. Time-of-use electricity price.

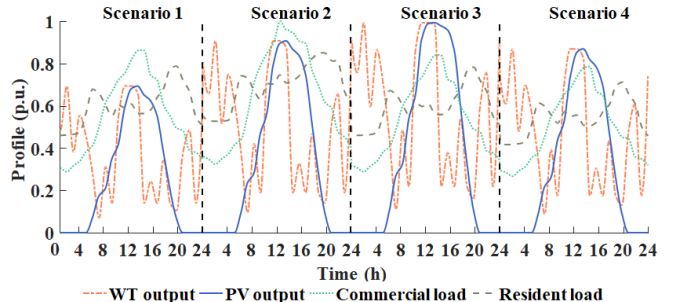


Fig. 7. Typical daily operational curves.

### B. Economic Analysis of Planning Results

Two cases are adopted to analyze the performance of the asymmetric bargaining-based planning method for SOPs.

Case I: Without SOP planning, each area trades only with the upper grid, and the initial operational state is obtained.

Case II: The SOP planning is implemented by adopting the proposed asymmetric bargaining-based planning method. Each area joins in P2P trading under the coordination of SOPs.

DISCO-1 is balanced in power supply and demand, while DISCO-2 has needs for DG consumption and DISCO-3 operates with heavy loads. Thus, as demonstrated in Fig. 8, DISCO-1 and DISCO-2 jointly supply power to DISCO-3 with a flexible configuration under Case II. The results show that a three-terminal SOP1 is planned among node 12, node 18, and node 32, whose capacity is 0.45, 0.65, and 1.10 MVA, respectively. A tie-line connected to node 38 is constructed and marked as a red line. SOP2 with a capacity of 0.40 MVA per terminal is planned between node 24 and node 35. The different capacities of multiple converters in SOP facilitate DISCOs to optimize their investments and get more benefits.

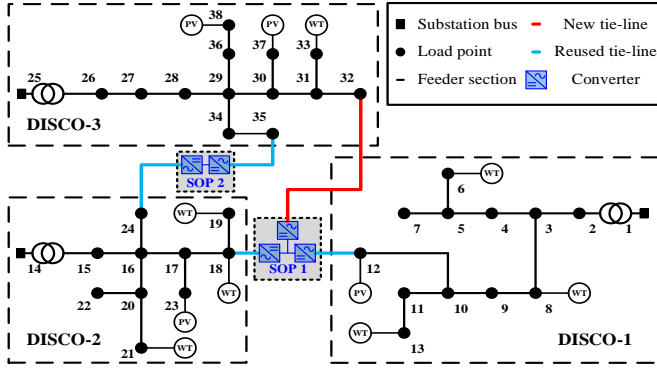


Fig. 8. Asymmetric bargaining-based planning results of SOPs under Case II.

TABLE III

INITIAL INVESTMENT COSTS UNDER CASE II

Cost (10 <sup>3</sup> CNY)	Stakeholder	DISCO-1	DISCO-2	DISCO-3
SOP investment		785.62	1020.94	1193.44
Tie-line construction		0	0	550.00
Land expropriation		1071.30	1827.10	2101.60
<b>Total</b>		<b>1856.92</b>	<b>2848.04</b>	<b>3845.04</b>

Table III presents the initial investment costs of each stakeholder, which are calculated as follows.

$$C^{\text{COST,SOP}} = \sum_{m \in \Omega^{\text{SOP}}} \sum_{i \in \Omega_m^{\text{AC}}} C^{\text{AC}}_{S_{m,i}}{}^{\text{SOP}} \quad (38.a)$$

$$C^{\text{COST,Line}} = \sum_{k \in \Omega^{\text{R}}} \sum_{ij \in \Omega_k^{\text{SOP,Line}}} \Psi C^{\text{L}}_{ij} \quad (38.b)$$

$$C^{\text{COST,S}} = \sum_{k \in \Omega^{\text{R}}} \sum_{m \in \Omega_k^{\text{SOP}}} C_m^{\text{site}} \quad (38.c)$$

As can be seen in Tables III and IV, DISCO-3 exhibits the strongest investment desire among all DISCOs. This heightened interest is driven by P2P trading, which allows DISCO-3 to acquire electricity from areas with a surplus, leading to a sizable reduction in annual total costs. The substantial reduction in total cost facilitates the investment of multiple DISCOs.

TABLE IV

INVESTMENT RATIO BARGAINING UNDER CASE II

Device	Stakeholder	DISCO-1	DISCO-2	DISCO-3
SOP1		0.3571	0.2901	0.3528
SOP2		-	0.4784	0.5216

To analyze the economic improvements of DNs under Case II, each cost of DISCOs under Cases I and II are presented in Table V. It is evident that the proposed method is effective in reducing the annual total cost of each DISCO. For DISCO-3, there has been a significant reduction in the cost of purchasing power from the upper grid, along with an improvement in voltage quality.

For both DISCO-1 and DISCO-2, participation in P2P trading is effective in facilitating renewable DG consumption, thereby leading to an improvement in voltage profile. Furthermore, DISCO-1 and DISCO-2 can make revenue by selling electricity in the P2P market. This profitability from the SOP installation drives the participation of all DISCOs.

TABLE V

EACH COST OF DISCOs UNDER CASES I AND II

Case	Category	Annual cost (10 <sup>3</sup> CNY)	DISCO-1	DISCO-2	DISCO-3
I	Operation	Trading with upper grid	4909.14	4998.63	14749.07
		Voltage deviation	0.26	126.14	6114.36
	<b>Total</b>	<b>4909.40</b>	<b>5124.77</b>	<b>20863.43</b>	
	Investment	Trading with upper grid	5393.78	6202.40	12208.90
P2P trading		-670.94	-1429.81	2834.25	
Voltage deviation		0.23	21.46	1360.97	
II	Operation	Cooperative surplus	-204.91	-242.86	-285.73
		SOP maintaining	7.86	10.21	11.93
		SOP investment	80.02	103.98	121.55
	Investment	Tie-line construction	0	0	56.02
Land expropriation		109.11	186.09	214.05	
<b>Total</b>		<b>4715.15</b>	<b>4851.47</b>	<b>16521.94</b>	
<b>Cost decrease ratio</b>			<b>3.96%</b>	<b>5.33%</b>	<b>20.81%</b>

Fig. 9 reveals an attractive return on investment for DISCOs under Case II, the more the DISCO invests, the more it wins. Note that the payback period is less than 5 years for each DISCO, which also means DISCOs are profitable for at least 75% of the time over the SOP lifetime. Thus, all DISCOs are keen to invest in the local energy market under Case II.

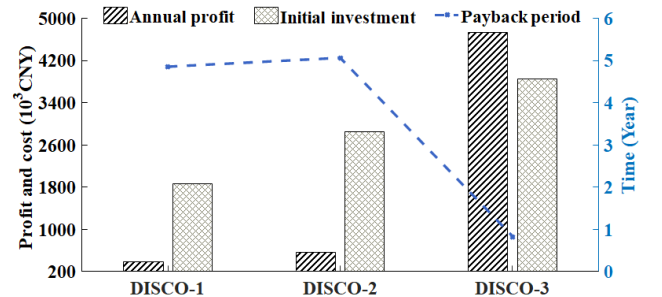


Fig. 9. Investment on return of DISCOs under Case II.

To illustrate the voltage improvement of DISCOs, the voltage profiles comparison at 10:00 am during scenario 3 under Cases I and II is given in Fig. 10. After the trading adjustments under Case II, the nodal voltage of the

distribution networks is basically within the desired voltage interval. The significant improvement in voltage quality of DISCO-3 is attributed to the active and reactive power injection facilitated by P2P electricity trading.

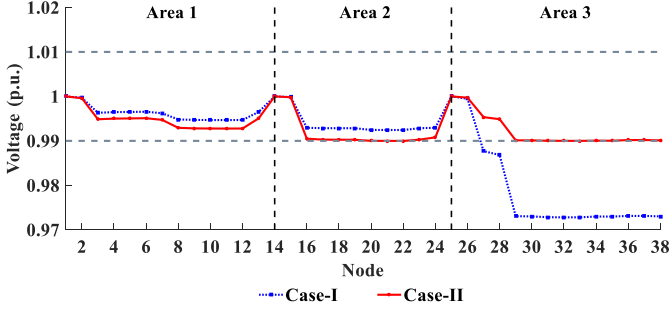


Fig. 10. Voltage profiles at 10:00 am during scenario 3 under Cases I and II.

### C. Comparison with Existing Studies

To further verify the effectiveness of the proposed planning method for SOPs, Case III is introduced for comparison.

Case III: Without game theory, an alliance is formed by all DISCOs. SOPs are planned to minimize the sum cost of the alliance, and no P2P payment among DISCOs [37].

In terms of economic comparison, the cost comparison under different cases is listed in Table VI. The results of Table VI show that the planning of SOPs under Case III reduces the total cost of DISCO-3 compared to Cases I and II. However, the increased total costs of DISCO-1 and DISCO-2 have caused a negative cost reduction ratio, which is unacceptable when each DISCO is regarded as an individual stakeholder. Moreover, without adopting game theory, the investment costs of SOPs and tie-lines are evenly shared by all DISCOs under Case III, which ignores the interests of different DISCOs. Comparatively, the implementation of game planning and P2P trading under Case II prevents DISCO-1 and DISCO-2 from unprofitable situations. Driven by profits from P2P payment, DISCOs flexibly invest in SOPs that are more beneficial to them when participating in the bargaining under Case II.

In terms of convergence comparison, the iterative process of ADMM under Case II is given in Fig. 11. The bargaining of the SOP planning scheme satisfies the stopping criterion after 4 iterations. During each round of the bargaining process, DISCOs consistently adjust their SOP planning schemes in response to the decisions made by the others involved. Besides, Fig. 12 presents the changes in the Lagrangian multiplier  $\lambda_{k,m}^{CAP}$  when planning SOP terminal connected to Node 18 during the bargaining process. As can be seen from Fig. 12, with an increasing number of iterations, the changes in  $\lambda_{k,m}^{CAP}$  tends to

flatten out. This also indicates that the bargaining is approaching equilibrium.

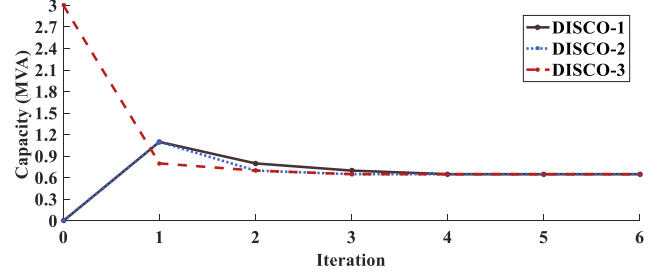


Fig. 11. Game process when planning SOP terminal connected to Node 18.

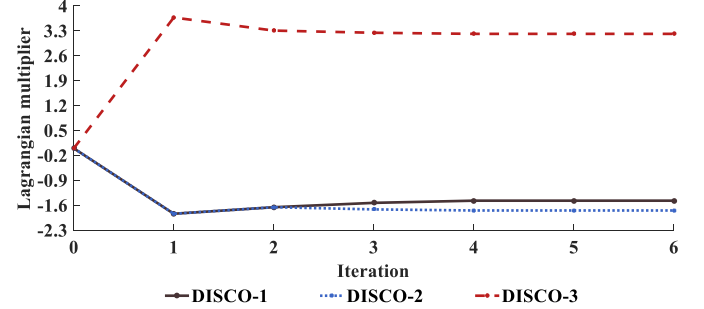


Fig. 12. Changes in  $\lambda$  when planning SOP terminal connected to Node 18.

Furthermore, Fig. 13 illustrates the variation of the upper and lower bounds during the iterations by applying the GBD algorithm. During the iterations, note that 6 Benders cuts are generated as new constraints for the master problem, with an increase in the lower bound. As the number of iterations increases, the upper bound of the master-problem presents a decreasing trend, while the lower bound gradually converges to the upper bound. Finally, the difference between the upper and lower bounds converges to zero at the 18th iteration, which means the successful convergence of GBD algorithm.

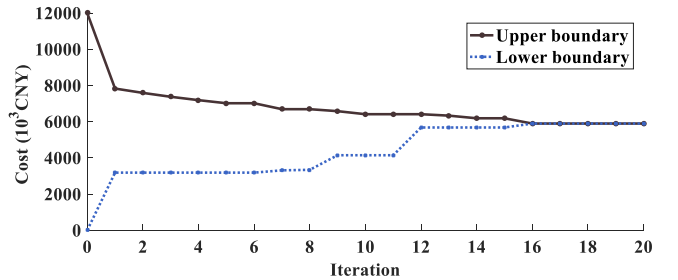


Fig. 13. Changes in  $\lambda$  when planning SOP terminal connected to Node 18.

In terms of computational time comparison, Table VII shows the computational time of different cases. Different from the real-time control, the operational state and the payback time of devices need to be measured in the planning,

TABLE VI  
COST COMPARISON UNDER DIFFERENT CASES

Case	SOP location (MVA)	Annual total costs of DISCOs ( $10^3$ CNY)								
		DISCO-1			DISCO-2			DISCO-3		
		Investment	Operation	Cost decrease ratio	Investment	Operation	Cost decrease ratio	Investment	Operation	Cost decrease ratio
I	-	-	4909.40	-	-	5124.77	-	-	20863.43	-
II	12 (0.45)-18 (0.65)-38 (1.1); 24 (0.4)-35 (0.4)	189.13	4526.02	3.96%	290.07	4561.40	5.33%	391.62	16130.32	20.81%
III	12 (2.1)-18 (2.1)-35 (2.1)	327.63	9421.17	-98.57%	327.63	6970.87	-42.42%	327.63	7727.79	61.39%

resulting in a consideration of long timescales for the planning model. Besides, note that the daily operating costs and the investment costs are usually converted into an annual total cost to analyze the return on investment in planning. Therefore, the computational time of the proposed method is sufficient to meet the planning demands.

TABLE VII  
COMPUTATIONAL TIME UNDER DIFFERENT CASES

Case	Computational time (s)
I	73.20
II	39615.23
III	2251.59

#### D. Scalability Analysis

To verify the scalability of the proposed method, Cases I and II are adopted in a modified practical DN [37] for analysis. The system contains six areas with a rated voltage level of 11.40 kV. The residential areas are managed by three stakeholders, DISCO-2, DISCO-4 and DISCO-6. And the remaining three commercial areas are operated by DISCO-1, DISCO-3 and DISCO-5, respectively. The total active and reactive power demands are 15.99 MW and 11.67 Mvar, respectively. Capacities of PV and WT arrays are 600 kVA and 800 kVA, respectively. There are ten nodes connected to tie-switches, which are marked by red points in Fig. 14.

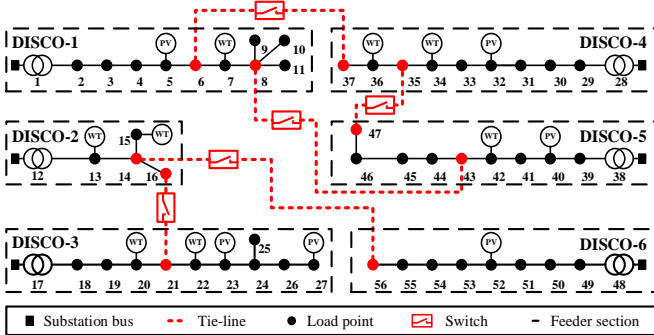


Fig. 14. Structure of the modified practical DNs with six areas.

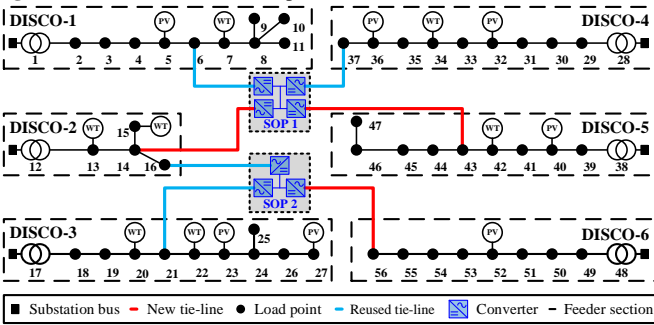


Fig. 15. Planning results in six-area DNs.

TABLE VIII  
COST COMPARISON OF DISCOS UNDER CASES I AND II

Case	SOP location (MVA)	Annual total cost of DISCOS ( $10^3$ CNY)					
		DISCO-1	DISCO-2	DISCO-3	DISCO-4	DISCO-5	DISCO-6
I	-	8050.50	1884.36	3898.21	3197.57	1395.36	8148.55
II	6(0.4)-14(0.6)- 37(0.6)-43(0.6);	7504.44	1588.02	3808.83	3052.73	1235.85	7687.14
	16(0.4)-21(1.0)- 56(1.4)						
<b>Cost decrease ratio</b>		<b>546.06</b>	<b>296.34</b>	<b>89.38</b>	<b>144.84</b>	<b>159.51</b>	<b>461.41</b>

As illustrated in Fig. 15, two SOPs are planned to realize the connection of six regional DNs. Table VIII presents the

annual total cost of the six DISCOs under Cases I and II. As can be observed from Table VIII, DISCOs can reduce the total costs by investing flexibly in SOPs. The implementation of P2P trading allows DISCOs to benefit from power exchanges. With the expansion of DNs, the proposed method remains applicable, ensuring the scalability for large-scale systems.

The above analysis shows that driven by the benefits of P2P trading, DISCOs are incentivized to assist each other in improving voltage quality. By applying the asymmetric bargaining method to deal with the planning and investment conflicts among multi-stakeholders, a mutually beneficial situation is achieved among DISCOs.

## VII. CONCLUSIONS

To address the optimal SOP configuration under multi-stakeholder investment, this paper proposes an asymmetric bargaining-based planning method for SOPs considering P2P trading. In this method, a two-layer coupling framework is established that integrates the planning, operation, and trading processes of multiple DISCOs. In the planning layer, the planning and investment scheme of SOPs is determined based on asymmetric bargaining. In the operational layer, P2P electricity trading is applied to facilitate economic operation of multiple DISCOs. The results show that the proposed method can effectively promote multi-stakeholders to invest in SOPs by balancing the interests of different stakeholders. Additionally, driven by P2P trading, the operational costs of DISCOs have been significantly reduced and the potential of SOPs in the local energy market has been well explored.

For the future, there are several notable directions to be explored. To avoid the investment reset and to increase the device utilization, future studies could focus on the optimization of installation time in the SOP planning. Besides, the game theory could be introduced into both the planning and operational layers to better describe the behaviour of multi-stakeholders.

## APPENDIX

### A. ADMM-based distributed algorithm

#### Algorithm 1 ADMM-Based Distributed Algorithm

- 1: **Initialize:** The decision variables  $M$ , the auxiliary variable  $\hat{M}$ , the penalty parameter  $\rho$ .
- 2: **Initial step:** Set the maximum number of iterations  $Z^{\max} = 300$ , the predefined accuracy  $\xi = 5 * 10^{-3}$ , the iteration index  $Z = 0$ , the Lagrangian multiplier  $\lambda = 0$ .
- 3: **While**  $\max(M(Z) - \hat{M}(Z)) \leq \xi$  or  $Z \leq Z^{\max}$  **do**  
 Based on the  $M$  made by DISCOs from the last iteration, update the set of decision strategies at fixed intervals;
- 4: **Each DISCO:** According to the  $\hat{M}(Z)$  obtained, determine its  $M(Z)$ ;
- 5:  $Z = Z + 1$ ;
- 6: Update  $\lambda(Z + 1)$  of each stakeholder;
- 7: **end**

In particular, to improve the calculation efficiency and accuracy of ADMM, the set of strategies is updated at fixed intervals during each iteration.

### B. GBD-based distributed algorithm

#### Algorithm 2 GBD-Based Distributed Algorithm

---

Initialize the iteration index  $Z_2 = 1$ , the maximum number of iterations  $Z_2^{\max} = 100$ .  $\Lambda^U$  and  $\Lambda^L$  are set to  $+\infty$  and  $-\infty$ , respectively.

2: **While**  $\Lambda^U - \Lambda^L < \xi_2$  or  $Z_2 \leq Z_2^{\max}$  **do**

3:   **MP**: obtain the optimal solution  $F^{\text{MP}}$  by (34), and update  $\Lambda^L = \max(\Lambda^L, F^{\text{M}})$ ;

4:   **SPs**: Obtain the optimal solution  $F_\omega^{\text{SP}}$  by solving the **SP** during each scenario;

5:   **If**  $F_\omega^{\text{SP}} > \Lambda_\omega, \omega \in N^{\text{TS}}$

6:     1) Generate the Benders cuts as shown in (B1.1);

7:     2) Add the Benders cuts (B1.1) to (35);

8:   **else**

9:     Break;

10:   **end**

11:   Update  $\Lambda^U$  according to (B1.2);

12:   Set  $Z_2 = Z_2 + 1$ ;

13: **end**

---

The Benders cuts are built in (B1.1), and  $\Lambda^U$  is updated according to (B1.2).

$$\Lambda_\omega \geq F_\omega^{\text{SP}} + \sum_{n=1}^{N_1} \tau_{\omega,n}^T g_{\omega,n}(x - \hat{x}) \quad (\text{B1.1})$$

$$\Lambda^U = \min\{\Lambda^U, a^T \hat{x} + \sum_{\omega=1}^{N^{\text{TS}}} (\sum_{n=1}^{N_1} \tau_{\omega,n}^T g_{\omega,n} \hat{x}_n + \sum_{n=1}^{N_2} o_{\omega,n}^T w_{\omega,n} + \sum_{n=1}^{N_3} r_{\omega,n}^T h_{\omega,n}) p_\omega\} \quad (\text{B1.2})$$

### C. Proof of the solution results

The optimality of the solution is proved by contradiction. For notational simplicity, assume that  $C_k = C_k^1 + C_k^{\text{Line}} + C_k^{\text{S}} + C_k^{\text{O}} + C_k^{\text{G}} + C_k^{\text{U}}$  and  $\pi_k = -R_k^{\text{P}} + C_k^{\text{P2P}}$ .

Firstly, let  $\{C'_k, \pi'_k, k \in \Omega^{\text{R}}\}$  be obtained from the solution. Suppose that the obtained solution  $F_k^{\text{DN}}, k \in \Omega^{\text{R}}$  is not the optimal solution and there exists  $F_k^{\text{DN}^*}, k \in \Omega^{\text{R}}$  such that  $\sum_{k \in \Omega^{\text{R}}} F_k^{\text{DN}^*} < \sum_{k \in \Omega^{\text{R}}} F_k^{\text{DN}}$ . Let  $\Delta F_k^{\text{DN}} = F_k^{\text{DN}^*} - F_k^{\text{DN}}$ , it is easy to infer the inequality as shown in (C1).

$$\sum_{k \in \Omega^{\text{R}}} \Delta F_k^{\text{DN}} < 0 \quad (\text{C1})$$

Thereby, it can be considered  $C_k = C'_k + \Delta F_k^{\text{DN}}$  for  $k = 1, \dots, N$  and  $\pi'_k = \pi_k - \Delta F_k^{\text{DN}}$  for  $k = 1, \dots, (N-1)$  and  $\pi'_N = \pi_N - \Delta F_N^{\text{DN}} + \varepsilon$ . Then, plugging in  $C_k$  and  $\pi_k$ , as can be shown in (C2).

$$\begin{aligned} & \prod_{k=1}^N [f_k^{\text{DN},0} - (C_k + \pi_k)]^{\tau_k} = \\ & [f_N^{\text{DN},0} - (C'_N + \Delta F_N^{\text{DN}} + \pi'_N - \Delta F_N^{\text{DN}} + \varepsilon)]^{\tau_N} * \\ & \prod_{k=1}^{N-1} [f_k^{\text{DN},0} - (C'_k + \Delta F_k^{\text{DN}} + \pi'_k - \Delta F_k^{\text{DN}})]^{\tau_k} \quad (\text{C2}) \\ & = [f_N^{\text{DN},0} - (C'_N + \pi'_N + \varepsilon)]^{\tau_N} \prod_{k=1}^{N-1} [f_k^{\text{DN},0} - \\ & (C'_k + \pi'_k)]^{\tau_k} \end{aligned}$$

From (14.a) and (C1), it can be conducted that  $\varepsilon = \sum_{k \in \Omega^{\text{R}}} \Delta F_k^{\text{DN}} < 0$ . Thus, (C3) can be obtained.

$$\prod_{k=1}^N [f_k^{\text{DN},0} - (C_k + \pi_k)]^{\tau_k} > \prod_{k=1}^N [f_k^{\text{DN},0} - (C'_k + \pi'_k)]^{\tau_k} \quad (\text{C3})$$

This contradicts that  $C'_k$  and  $\pi'_k$  maximize the planning model. Therefore, the obtained solution  $C'_k$  and  $\pi'_k$  is the optimal solution and the proof is complete.

### REFERENCES

- [1] Y. Wang, J. Qiu and Y. Tao, "Robust energy systems scheduling considering uncertainties and demand side emission impacts", *Energy*, vol. 239, pp. 122317, Jan. 2022.
- [2] Y. Shen, S. Zhang, M. Ding, H. Cheng, C. Li and D. Liu, "Expansion planning of soft open points based distribution system considering EV traffic flow", *IEEE Trans. Ind. Appl.*, vol. 60, no. 1, pp. 1229-1239, Jan. 2024.
- [3] Y. Xia, Q. Xu, J. Fang and F. Li, "Non-iterative decentralized peer-to-peer market clearing in multi-microgrid systems via model substitution and network reduction", *IEEE Trans. Power Syst.*, vol. 39, no. 2, pp. 2922-2935, Mar. 2024.
- [4] W. Wang, G. Tian, Q. Sun and H. Liu, "A control framework to enable a commercial building HVAC system for energy and regulation market signal tracking", *IEEE Trans. Power Syst.*, vol. 38, no. 1, pp. 290-301, Jan. 2023.
- [5] J. Jian, J. Zhao, H. Ji, L. Bai, J. Xu, P. Li, J. Wu and C. Wang, "Supply restoration of data centers in flexible distribution networks with spatial-temporal regulation", *IEEE Trans. Smart Grid*, vol. 15, no. 1, pp. 340-354, Jan. 2024.
- [6] X. Jiang, Y. Zhou, W. Ming, P. Yang and J. Wu, "An overview of soft open points in electricity distribution networks", *IEEE Trans. Smart Grid*, vol. 13, no. 3, pp. 1899-1910, May. 2022.
- [7] M. Ullah and J. Park, "Peer-to-peer energy trading in transactive markets considering physical network constraints", *IEEE Trans. Smart Grid*, vol. 12, no. 4, pp. 3390-3403, Jul. 2021.
- [8] L. Wang, Q. Zhou, Z. Xiong, Z. Zhu, C. Jiang, R. Xu and Z. Li, "Security constrained decentralized peer-to-peer transactive energy trading in distribution systems", *CSEE J. Power Energy Syst.*, vol. 8, no. 1, pp. 188-197, Jan. 2022.
- [9] X. Yang, Z. Song, J. Wen, L. Ding, M. Zhang, Q. Wu and S. Cheng, "Network-constrained transactive control for multi-microgrids-based distribution networks with soft open points", *IEEE Trans. Sustain. Energy*, vol. 14, no. 3, pp. 1769-1783, Jul. 2023.
- [10] N. Nasiri, S. Zeynali, S. Ravadanegh and S. Kubler, "Moment-based distributionally robust peer-to-peer transactive energy trading framework between networked microgrids, smart parking lots and electricity distribution network", *IEEE Trans. Smart Grid*, vol. 15, no. 2, pp. 1965-1977, Mar. 2024.
- [11] Y. Zou, Y. Xu, X. Feng and H. Nguyen, "Peer-to-peer transactive energy trading of a reconfigurable multi-energy network", *IEEE Trans. Smart Grid*, vol. 14, no. 3, pp. 2236-2249, May. 2023.
- [12] A. Najafi, M. Pourakbari-Kasmaei, M. Jasinski, J. Contreras, M. Lehtonen and Z. Leonowicz, "The role of EV based peer-to-peer transactive energy hubs in distribution network optimization", *Appl. Energy*, vol. 319, pp. 119267, Aug. 2022.
- [13] C. Zhang, Y. Yang, Y. Wang, J. Qiu and J. Zhao, "Auction-based peer-to-peer energy trading considering echelon utilization of retired electric vehicle second-life batteries", *Appl. Energy*, vol. 358, pp. 122592, Mar. 2024.
- [14] X. Yan, M. Song, J. Cao, C. Gao, X. Jing, S. Xia and M. Ban, "Peer-to-peer transactive energy trading of multiple microgrids considering renewable energy uncertainty", *Int. J. Electr. Power Energy Syst.*, vol. 152, pp. 109235, Oct. 2023.
- [15] J. Li, M. Khodayar, J. Wang and B. Zhou, "Data-driven distributionally robust co-optimization of P2P energy trading and network operation for interconnected microgrids", *IEEE Trans. Smart Grid*, vol. 12, no. 6, pp. 5172-5184, Nov. 2021.
- [16] H. Ji, J. Jian, H. Yu, J. Ji, M. Wei, X. Zhang, P. Li, J. Yan and C. Wang, "Peer-to-peer electricity trading of interconnected flexible distribution networks based on distributed ledger", *IEEE Trans. Ind. Inform.*, vol. 18, no. 9, pp. 5949-5960, Sep. 2022.
- [17] V. Pamshetti, S. Singh, A. Thakur, S. Singh, T. Babu, N. Patnaik and G. Krishna, "Cooperative operational planning model for distributed energy resources with soft open point in active distribution network", *IEEE Trans. Ind. Appl.*, vol. 59, no. 2, pp. 2140-2151, Mar. 2023.
- [18] J. Wang, N. Zhou, C. Chung and Q. Wang, "Coordinated planning of converter-based DG units and soft open points incorporating active

management in unbalanced distribution networks”, *IEEE Trans. Sustain. Energy*, vol. 11, no. 3, pp. 2015-2027, Jul. 2020.

- [19] Y. He, H. Wu, R. Bi, R. Qiu, M. Ding, M. Sun, B. Xu and L. Sun, “Coordinated planning of distributed generation and soft open points in active distribution network based on complete information dynamic game”, *Int. J. Electr. Power Energy Syst.*, vol. 138, pp. 107953, Jan. 2022.
- [20] L. Ali, S. Muyeen, H. Bizhani and M. Simoes, “Economic planning and comparative analysis of market-driven multi-microgrid system for peer-to-peer energy trading”, *IEEE Trans. Ind. Appl.*, vol. 58, no. 3, pp. 4025-4036, May. 2022.
- [21] A. Nazari, R. Keypour and N. Amjadi, “Joint investment of community energy storage systems in distribution networks using modified Nash bargaining theory”, *Appl. Energy*, vol. 301, pp. 117475, Jul. 2021.
- [22] M. Khorasany, A. Paudel, R. Razzaghi and P. Siano, “A new method for peer matching and negotiation of prosumers in peer-to-peer energy markets”, *IEEE Trans. Smart Grid*, vol. 12, no. 3, pp. 2472-2483, May, 2021.
- [23] M. Ullah and J. Park, “Transactive energy market operation through coordinated TSO-DSOs-DERs interactions”, *IEEE Trans. Power Syst.*, vol. 38, no. 2, pp. 1978-1990, Mar. 2023.
- [24] W. Zhang, B. Zheng, W. Wei, L. Chen and S. Mei, “Peer-to-peer transactive mechanism for residential shared energy storage”, *Energy*, vol. 246, pp. 123204, May. 2022.
- [25] H. Sheng, C. Wang, X. Dong, K. Meng and Z. Dong, “Incorporating P2P trading into DSO’s decision-making: a DSO-prosumers cooperated scheduling framework for transactive distribution system”, *IEEE Trans. Power Syst.*, vol. 38, no. 3, pp. 2362-2375, May. 2023.
- [26] X. Chang, Y. Xu and H. Sun, “Vertex scenario-based robust peer-to-peer transactive energy trading in distribution networks”, *Int. J. Electr. Power Energy Syst.*, vol. 138, pp. 107903, Jun. 2022.
- [27] M. Yan, M. Shahidehpour, A. Paaso, L. Zhang, A. Alabdulwahab and A. Abusorrah, “Distribution network constrained optimization of peer-to-peer transactive energy trading among multi-microgrids”, *IEEE Trans. Smart Grid*, vol. 12, no. 2, pp. 1033-1047, Mar. 2021.
- [28] I. Alkhouri, A. Awad, Q. Sun and G. Atia, “Imperceptible attacks on fault detection and diagnosis systems in smart buildings”, *IEEE Trans. Ind. Inform.*, vol. 20, no. 2, pp. 8125-8137, Feb. 2024.
- [29] Y. Xia, Q. Xu, Y. Ding, L. Shi and F. Wu, “Generalized Nash equilibrium analysis for peer-to-peer transactive energy market considering coupling distribution network constraints”, *IEEE Trans. Ind. Inform.*, vol. 20, no. 6, pp. 8125-8137, Jun. 2024.
- [30] S. Cui, Y. Wang, X. Liu, Z. Wang and J. Xiao, “Economic storage sharing framework: asymmetric bargaining-based energy cooperation”, *IEEE Trans. Ind. Inform.*, vol. 17, no. 11, pp. 7489-7500, Nov. 2021.
- [31] T. Zhang, C. Chen, L. Ma, T. Chen, Y. Wei, Z. Lin and D. Srinivasan, “Multi-step clustering and generalized Nash bargaining-based planning strategy of community-shared energy storage for large-scale prosumers”, *IEEE Trans. Sustain. Energy*, vol. 15, no. 2, pp. 1013-1027, Apr. 2024.
- [32] H. Zhang, S. Zhou, W. Gu, C. Zhu and X. Chen, “Optimal operation of micro-energy grids considering shared energy storage systems and balanced profit allocations”, *CSEE J. Power Energy Syst.*, vol. 9, no. 1, pp. 254-271, Jan. 2022.
- [33] L. Han, T. Morstyn and M. McCulloch, “Incentivizing prosumer coalitions with energy management using cooperative game theory”, *IEEE Trans. Power Syst.*, vol. 34, no. 1, pp. 303-313, Jan. 2019.
- [34] N. Liu, X. Yu, C. Wang, C. Li, L. Ma and J. Lei, “Energy-sharing model with price-based demand response for microgrids of peer-to-peer prosumers”, *IEEE Trans. Power Syst.*, vol. 32, no. 5, pp. 3569-3583, Sep. 2017.
- [35] Z. Lu, J. Wang, M. Shahidehpour, L. Bai, Z. Li, L. Yan and X. Chen, “Risk-aware flexible resource utilization in an unbalanced three-phase distribution network using SDP-based distributionally robust optimal power flow”, *IEEE Trans. Smart Grid*, vol. 15, no. 3, pp. 2553-2569, May. 2024.
- [36] A. Rodriguez and A. Laio, “Clustering by fast search and find of density peaks”, *Science*, vol. 344, no. 6191, pp. 1492-1496, Jun. 2014.
- [37] C. Wang, G. Song, P. Li, H. Ji, J. Zhao and J. Wu, “Optimal siting and sizing of soft open points in active electrical distribution networks”, *Appl. Energy*, vol. 189, pp. 301-309, Mar. 2017.



China National Postdoctoral Program for Innovative Talents.



**Haoran Ji** (Senior Member, IEEE) received the B.S. and Ph.D. degrees in electrical engineering from Tianjin University, Tianjin, China, in 2014 and 2019, respectively.

From 2019 to 2021, he was a Postdoctoral Research with Tianjin University. He is currently an Associate Professor with Tianjin University. His research interests include distributed generation systems and optimal operation of distribution networks. He was supported by

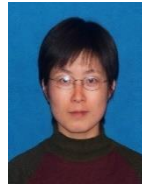
**Yuxin Zheng** received the B.S. degree in electrical engineering from Tianjin University, Tianjin, China, in 2022. He is currently working toward the M.S. degree in electrical engineering with Tianjin University, Tianjin, China.

His current research interests include optimal planning of distribution networks.



**Hao Yu** (Senior Member, IEEE) received the B.S. and Ph.D. degrees in electrical engineering from Tianjin University, Tianjin, China, in 2010 and 2015, respectively. He is currently an Associate Professor with the School of Electrical and Information Engineering, Tianjin University.

His current research interests include the operation analysis and optimization of active distribution networks and integrated energy systems. He is the assistant editor of IET Energy Systems Integration.



**Jinli Zhao** (Member, IEEE) received the Ph.D. degree in electrical engineering from Tianjin University, Tianjin, China, in 2007. She is currently an Associate Professor in the School of Electrical and Information Engineering, Tianjin University.

Her research interests include operation and planning of active distribution networks, and power system security and stability.



**Guanyu Song** (Senior Member, IEEE) received the B.S. and Ph.D. degrees in electrical engineering from Tianjin University, Tianjin, China, in 2012 and 2017, respectively.

He is currently a Senior Engineer with the School of Electrical and Information Engineering, Tianjin University. His current research interests include optimal planning and operation of smart distribution system.



**Jianzhong Wu** (Fellow, IEEE) received the B.Sc., M.Sc., and Ph.D. degrees in electrical engineering from Tianjin University, China, in 1999, 2002 and 2004, respectively.

From 2004 to 2006, he was at Tianjin University, where he was an Associate Professor. From 2006 to 2008, he was a Research Fellow at the University of Manchester, Manchester, U.K. He is a Professor of Multi-Vector Energy Systems and the Head of the School of Engineering, Cardiff University, U.K. His research interests include integrated multi-energy infrastructure and smart grid. He is

Co-Editor-in Chief of Applied Energy. He is the Co-Director of U.K. Energy Research Centre and EPSRC Supergen Energy Networks Hub.



**Peng Li** (Senior Member, IEEE) received the B.S. and Ph.D. degrees in electrical engineering from Tianjin University, Tianjin, China, in 2004 and 2010, respectively.

He is currently a Professor with the School of Electrical and Information Engineering, Tianjin University. His current research interests include operation and planning of active distribution networks, modeling, and transient simulation of power systems. Prof. Li is an Associate Editor of IEEE Transactions on Sustainable Energy, CSEE

Journal of Power and Energy Systems, Sustainable Energy Technologies and Assessments, and IET Renewable Power Generation.